ERICE PREPRINT SERIES

«ETTORE MAJORANA» CENTRE FOR SCIENTIFIC CULTURE

EMCSC/ELN 93-01
10 February 1993

HADRON DISTRIBUTIONS IN THE FINAL STATE OF DIS AT HERA

A.V. Anisovich, G. Anzivino, F. Arzarello, Ya.I. Azimov, G. Bari, M. Basile, L. Bellagamba, D. Boscherini, G. Bruni, P. Bruni, G. Cara Romeo, M. Chiarini, L. Cifarelli, F. Cindolo, F. Ciralli, A. Contin, S. D'Auria, C. Del Papa, S. De Pasquale, F. Fiori, F. Frasconi, P. Giusti, G. Iacobucci, G. Maccarrone, A. Margotti, T. Massam, R. Nania, F. Palmonari, S. Qian, G. Sartorelli, M. Schioppa, S.Yu. Sivoklokov, G. Susinno, R. Timellini, L. Votano and A. Zichichi

CERN, Geneva, Switzerland
INFN, Eloisatron Project, Erice, Italy
INFN, Bologna, Italy
INFN, LNF, Frascati, Italy
Nuclear Physics Institute, Moscow State University, Moscow, Russia
Physics Department, University of Bologna, Italy
Physics Department, University of Calabria, Cosenza, Italy
Physics Department, University of Pisa, Italy
PNPI, Gatchina, St. Petersburg, Russia
World Laboratory, Lausanne, Switzerland

Abstract

Momentum distributions of secondary hadrons produced in deep inelastic scattering (DIS) are studied for both current and target fragmentation regions. They are shown to contain interesting information on several important questions of hadroproduction dynamics such as target structure and hadronization mechanism. Special emphasis is given to the HERA kinematical region.

(Submitted to Il Nuovo Cimento)

1. INTRODUCTION

Since the very beginning of its study, deep inelastic scattering (DIS) of leptons off hadrons has been considered as *the* classical example of hard process [1]. Its interpretation as point-like collision with a quark inside the hadron agrees very well with the behaviour of the corresponding cross-sections. Large additional (and much more detailed) information both on the process itself and on the quark-gluon structure of the target hadron may be obtained by measuring hadrons in the DIS final state. Their distributions at large Q and 1/x reflect, in particular, the space-time picture of the process (see [2, 3]). Of great interest in this respect is the beginning of HERA operation which makes accessible a vast region of the (Q^2, x)-plane and opens new perspectives for QCD studies.

In the present paper, we focus on the HERA case and give theoretical predictions on the basic properties of multihadron final states. We consider the (fractional) momentum distributions of hadrons in the Breit reference system, where theoretical interpretation looks more transparent. The exchanged vector particle in this system has no energy. Its momentum, having absolute value Q, is opposite to the incoming hadron (target) momentum whose absolute value is:

$$P = Q/2x. \tag{1}$$

The first stage of DIS has a very simple interpretation in this system [1]: a quark is knocked out from the target and goes, with momentum Q/2, in the initial vector particle direction while target remnants conserve their initial motion (here and in what follows, we assume the knocked parton to be a quark). As usual we call the hemisphere in the direction of the initial vector particle the current fragmentation (CF) region, while the other hemisphere in the direction of the initial target hadron is called the target fragmentation (TF) region. For the two following stages of DIS, namely QCD cascading and hadronization, we use the results of perturbative QCD (PQCD) calculations [4, 5] and the hypothesis of local parton-hadron duality (LPHD) [6, 7].

The presentation goes as follows. In Sects. 2 and 3 we give predictions for hadron production in the current and in the target fragmentation regions, separately. The results obtained and their possible dependence on various physical assumptions are discussed in Sect. 4. In Sect. 5 we summarize our results and briefly mention some possibilities to check them experimentally.

2. CURRENT FRAGMENTATION

In the Breit system, the current fragmentation region (CF) looks very simple at the parton level: there is one outgoing quark with energy Q/2. This reminds very closely the

outgoing quark with energy W/2 in e^+e^- annihilation into hadrons. Then the quark produces cascades, mainly purely gluonic. The products of cascading constitute a jet made of particles whose energy distribution inside it is nearly insensitive to the parton structure in the target fragmentation (TF) region. Together with the LHPD hypothesis, this leads to the conclusion (e.g. [4, 5]) that the energy (or momentum) distribution of particles in the CF region of DIS should practically coincide with the one obtained in e^+e^- annihilation up to a factor 1/2 (one jet instead of two).

Let us discuss this point in some more detail. Previous experience shows that jets in e^+e^- annihilation become observable at $W \approx 7$ GeV. They are well separated at $W \geq 10$ GeV. Only then one is able to consider the independence (in any meaning of the word) of jets with respect to each other.

Let us now return to DIS. The value of Q plays in CF the same role as W in e^+e^- annihilation. So only at $Q^2 \geq 10^2$ GeV^2 a comparison of hadron distributions in CF and in e^+e^- is meaningful. In addition, if the CF jet is well separated from the TF jet(s), then hadron distributions inside it should be nearly independent of x, which can be measured experimentally.

Figure 1 shows the fractional momentum distributions relative to all charged hadrons produced in the CF jet at different Q^2. Our calculations are based on the modified leading logarithmic approximation (MLLA) [8, 9] that is known to work for e^+e^- annihilation in a wide energy interval, from $W \approx 10$ GeV up to the Z^0 peak [7, 10-12]. The variable used is:

$$y_p = \ln(2p_h/Q), \tag{2}$$

where p_h is the hadron momentum in the current fragmentation region. The above variable is analogous to:

$$\ln x_p = \ln(2p_h/W), \tag{3}$$

in the e^+e^- annihilation case and for the corresponding distributions we expect:

$$\frac{dn_h^{CF}(Q)}{dy_p} \approx \frac{1}{2}\frac{d\,n_h^{e^+e^-}(W)}{d\ln x_p}, \tag{4}$$

as mentioned above. For the two parameters of MLLA description (Λ_{eff}, an effective QCD scale parameter, and K, an overall normalization factor of the hadron distribution accounting for parton-hadron transition), we take the values $\Lambda_{eff} = 250$ MeV and $K = 1.3$ already used in [10] to fit charged hadron distributions in e^+e^- annihilation[1]. For all the curves in Fig. 1 and

---

1 This is why we consider the curves in Fig. 1 as the distributions of all charged hadrons. In the same way we can describe the distributions of all hadrons or of a particular kind of them.

in the following we apply the restriction $p_h > 400$ MeV to reduce the vanishing of the dn_h/dy_p distributions when $p_h \to 0$, due to trivial phase-space effects.

As Q increases, the hadron yield increases and the curves in Fig. 1 reveal more and more the dynamical nature of their hump-backed shape. This is well known in e^+e^- annihilation and results from QCD coherence. Note that the CF region in DIS may be an even better QCD laboratory than the e^+e^- final state. In fact the CF jet may be studied at HERA up to $Q \approx 300$ GeV, while in e^+e^- annihilation, above the W^+W^- production threshold ($W \approx 160$ GeV), the study of quark jets may require a good handling of the non-negligible W^+W^- *background*. Moreover, e^+e^- annihilation needs special procedures to separate light and heavy quarks having somewhat different QCD radiation structures. The CF jet in DIS really contains only light quark contributions.

3. TARGET FRAGMENTATION

The structure of parton and, moreover, hadron distributions in the target fragmentation (TF) region is much more complicated than in the CF one. In particular, it essentially depends on x. At first sight this is trivial since valence and sea quark contributions, of course, should lead to different parton and hadron distributions in the final state, whose relative role should change with x. But the x-dependence of the final state conserves even for DIS off pure sea quarks.

The summation of large logarithmic terms in perturbative QCD (PQCD) enables one to study the final state structure in detail [4, 5]. Sea quarks that dominate the small x region are mainly pair produced at the last step of gluon cascading. The energy distribution of secondary particles appears to consist of three components. The first one is due to the radiation of the antiquark companion of the knocked out quark. The second one, to the soft coherent radiation from the gluon cascade (related to the quark-antiquark pair being in an octet colour state before the hard collision). At last, the third one corresponds to the fragmentation of *rungs* in the gluon cascade: it is sensitive to the detailed structure of the cascade.

Here we apply the explicit formulae of [4, 5] to calculate the expected momentum distributions in the TF region of DIS for Q^2 and x values within the HERA range, and even beyond, in order to illustrate some interesting trends.

For target fragmentation we use the same variable (2) as for current fragmentation. Such a choice looks strange and inconvenient at first sight. In particular y_p takes both positive and negative values in the TF region. But what makes it useful is that different mechanisms are expected to influence the particle distributions at $y_p > 0$ and $y_p < 0$: of the three contributions described above, the first two should be dominant for $y_p < 0$ while only

the third one should work for $y_p > 0$.

For most of the further calculations we adopt the S-DIS structure function parametrization of [13]. Figure 2 shows the y_p distributions of charged hadrons in the target fragmentation region obtained at three fixed values of Q^2 for different values of x. For each Q^2 value, we give three TF curves: these can be compared to each other and to the corresponding CF distribution, relative to the same Q^2 value (the CF curves superimposed in Fig. 2 are taken from Fig. 1). Figure 3 illustrates the Q^2-dependence of the TF distributions: it compares the curves with various Q^2 at fixed x.

4. PROPERTIES OF HADRON DISTRIBUTIONS

In this section we discuss the features of the distributions obtained so far. Let us start with the CF case. As already pointed out, the curves in Fig. 1 should be nearly equivalent to half the corresponding distributions for final hadrons in e^+e^- annihilation. Therefore, many well-known properties of e^+e^- may be applied to the CF region of DIS. However some properties are specific to DIS, first of all the presence of the x parameter having no analogue in e^+e^-. Simplest expectations predict x-independence for the CF distribution. But it is more probable that some x-dependence will appear. Let us discuss the main two reasons for this.

The first is related to the transverse initial motion of the quark which, surely, depends on x. It should produce some azimuthal asymmetry in CF hadron production and a deviation of the thrust axis in the CF hemisphere with respect to the exchanged vector particle direction. It can also produce mixing of the soft particles between the two CF and TF hemispheres and induce the x-dependence of their spectrum.

Another mechanism for x-dependence, acting again mainly on soft particles, is the coherence of soft particle production by CF and TF partons. It suppresses their production and at the same time makes the CF soft particle spectrum sensitive to the TF parton structure and, in particular, to x. The two mechanisms could be in principle separated by a combined use of both CF particle distributions and CF jet (as a whole) properties, such as energy, orientation and so on.

Hadron distributions in TF strongly depend on both Q^2 and x. The hadron yield increases if either Q^2 or 1/x increase. For fixed Q^2, the shape of the TF distribution has as pronounced peak whose position is x-independent and nearly the same as for the corresponding CF distribution (Fig. 2), i.e.

$$y_p^{(\max \text{ TF})} \approx y_p^{(\max \text{ CF})}. \qquad (5)$$

Clearly different behaviours show up for $y_p > 0$ and $y_p < 0$. When 1/x increases at fixed Q^2, the spectrum at $y_p < 0$ increases and makes the peak more and more pronouced (Fig. 2). But

near $y_p = 0$ the increase is much weaker. The main effect at $y_p > 0$ is the widening of the kinematical region and the development of a plateau-like structure with:

$$\frac{dn_h^{TF}(y_p)}{dy_p} \simeq \frac{dn_h^{TF}(0)}{dy_p} \tag{6}$$

in a wide interval of positive values of y_p.

When Q^2 increases at fixed x, the distribution widens in the negative direction and grows moderately at $y_p > 0$. It tends to produce a one-peak structure having a distorted gaussian-like shape (Fig. 3). The larger is 1/x, the later the point $y_p = 0$ ceases to be a characteristic point of the TF hadron distribution.

Our calculations are based on three main assumptions: i) the PQCD description of the cascading and fragmentation of partons; ii) the choice of a particular set of structure functions; iii) the local parton-hadron duality (LPHD) for hadronization. How reliable are they?

The PQCD approach has demonstrated its working abilities in various processes, especially in e^+e^- annihilation into hadrons. Essential deviations from its predictions would mean essential nonperturbative effects which, as such, would be interesting by themselves.

The description of nucleon structure functions will surely improve thanks to HERA experiments. Meanwhile we can try to estimate their influence on the results using different existing phenomenological parametrizations. For instance Fig. 4 compares two of the TF hadron distributions already shown in Fig. 3 to those obtained with another set of structure functions (GRV(HO) [14]). Despite the differences, the main features of the curves remain.

The hardest (and one of the most interesting) is the problem of the relationship between parton and hadron distributions that goes beyond perturbative calculations. The LHPD approach [4, 5] used in our calculations works quite well in e^+e^- for both momentum [7, 10-12] and angular distributions [15, 16]. But the parton structure of the TF region of DIS is much more complicated and may lead to unexpected nonperturbative phenomena.

The plateau of the secondary hadron distributions in the TF region (Figs. 2-4) can be considered as nonperturbative since phenomenological structure functions are used, which are of course beyond perturbative expansions. This plateau in DIS could be directly related to the central region plateau of high energy hadron-hadron collisions, just as gluon cascades at small x are likely related to Pomeron cuts. In addition, a sharp change in the particle spectrum at $y_p = 0$, as the one appearing in Fig. 4a, seems to indicate some mismatch between the gluon and sea quark structure function parametrizations. In fact, in a theory with possible soft radiation like QCD, smearing effects due to *radiative tails* should produce a sort of equilibrium between gluon and sea quark functions, which might not be fully accounted for in phenomenological approaches.

Another nonperturbative aspect is the transformation of final partons into hadrons. To study the effect of different hadronization mechanisms, we compare the TF hadron distributions of Figs. 2-3 with the results of Monte Carlo simulations performed with LEPTO 6.1 [17], which is based on the well-known string hadronization mechanism. We simulate ep collisions with S-DIS [13] structure functions as in Figs. 2-3. Figure 5 shows two examples of LEPTO-simulated y_p distributions relative to charged pions produced in the TF region, at fixed x and different Q^2 values. These should be compared[2] with the corresponding distributions of Fig. 3a. The distributions are quite similar (peak height and position) but two points should be noted: in Fig. 5 the histograms show a smoother behaviour at $y_p = 0$ and a weaker Q^2-dependence at $y_p > 0$. In Fig. 6 we show the Monte Carlo spectra obtained at fixed Q^2 and different x values, to be compared with those in Fig. 2a. Again the distributions are similar but in Fig. 6 the shapes are smoother and their changes more uniform. These features can be explained having in mind the string mechanism. Long range strings may connect partons from different kinematical regions and tend to attenuate any sharp change in the distribution shape.

If such explanation is correct, we should expect the strings to connect partons from the CF and TF regions. Since TF partons are more numerous and have higher momenta, the string hadronization should carry away particles and energy from the CF region. When 1/x increases, the number of TF partons with high momenta increases and the effect should be enhanced. Monte Carlo simulations indeed demonstrate this effect, as illustrated for instance in Fig. 7 where different CF distributions are shown for typical x and Q^2 values. When x decreases from 10^{-2} to 10^{-3} at fixed $Q^2 = 10^2$ GeV^2, the CF hadron distribution looses about 20 % of particles, nearly uniformly over y_p. Notice that the Q^2 evolution at fixed x of the histograms in Fig. 7 agrees with the expectations of local hadronization in Fig. 1.

5. SUMMARY AND CONCLUSIONS

Let us summarize our results and discuss the experimental possibilities to check them. First of all, it is useful to analyze the secondary hadrons of DIS in the Breit frame. HERA is the first facility where hadron production mechanisms in the current fragmentation (CF) and target fragmentation (TF) regions should become distinct enough, so that studying them separately will be possible.

The angular distribution of the CF jet axis should reveal the transverse motion of

---

2 The Monte Carlo spectra refer to charged pions, which represent the bulk of all charged particles (excluding some special kinematical region, such as the very forward region mainly containing leading protons). These can reasonably be compared to the charged hadron distributions obtained as described in Sects. 2 and 3. In fact the formulae used therein cannot pretend to describe leading protons.

quarks inside the proton. The fractional momentum ($y_p = \ln(2p_h/Q)$) distribution of CF hadrons is expected to be nearly the same as half the hadron distribution in e^+e^- annihilation at the corresponding energy ($W \approx Q$). Its x-dependence should be sensitive to the hadronization mechanism. Local hadronization leads to a weak x-dependence. String hadronization, with long range strings connecting different kinematical regions, enhances this dependence and washes away CF hadrons when x decreases.

The fractional momentum distribution of TF hadrons can be studied in terms of the same y_p variable. It should differently vary vs. Q^2 and x in the negative and positive y_p regions which should correspond to different contributions of hadroproduction dynamics. The peak positions of the CF and TF distributions should roughly be the same. The detailed structure of the TF distribution should be sensitive to the hadronization mechanism. Local hadronization predicts a plateau at positive y_p (likely related to the well-known plateau in hadron-hadron collisions), which develops as x decreases at fixed Q^2. String hadronization in the TF region tends to eliminate any flattening near $y_p = 0$, thus making the distribution at positive y_p values a smooth continuation of the one at negative values, and to influence the CF region, as already pointed out above.

Therefore we see three separate regions of interest for experimental studies: the CF region and the two TF regions at $y_p > 0$ and $y_p < 0$, respectively. Unfortunately the positive y_p region, where the plateau may be expected, is experimentally difficult because of the nonhermeticity of the detectors around the beam direction. At HERA, due to its asymmetric kinematics, only a small number of secondaries will escape through the detector hole around the outgoing electron beam direction but many more will do it on the outgoing proton side.

To illustrate this point, we again use Monte Carlo simulations with the parameters of the ZEUS detector at HERA, whose coverage extends down to 2.2° on the outgoing proton side and down to 3.5° on the outgoing electron side. The result is that the proton beam hole strongly absorbs TF hadrons with positive y_p values, as illustrated in Fig. 8. For instance, for $Q^2 = 10^2$ GeV^2 and $x = 10^{-3}$ the TF spectrum weakens ten times at $y_p = 3$, and for $Q^2 = 10^3$ GeV^2 and $x = 10^{-2}$ the same happens already at $y_p = 1$. Notice that the extreme positive y_p region is covered in the ZEUS detector by the leading proton spectrometer (LPS) whose role will be relevant in this context. The negative y_p region is much less affected by the proton beam hole while the CF region stays nearly untouched. Finally, concerning the electron beam hole, this absorbs only a small fraction of both CF and TF hadrons.

To conclude, in the present work we give perturbative QCD predictions for the fractional momentum distributions of secondary hadrons produced in DIS final states, separately for current and target fragmentation, in a range of x and Q^2 easily explorable at HERA. Secondary hadrons can be experimentally studied in at least two interesting kinematical regions. Their angular and momentum distributions will give important

contributions to the understanding of hadron production mechanisms, in particular in terms of proton structure and parton hadronization.

Acknowledgements

The authors are thankful to Yu.L. Dokshitzer, V.A. Khoze and M. Ryskin for very useful discussions.

REFERENCES

[1] R.P. Feynman: "Photon-Hadron Interactions" (Benjamin, 1972).

[2] V.N. Gribov: in Proceedings of the 8th Winter School of LNPI, Gatchina, Leningrad, USSR, 1973 (LNPI, 1973), vol. 2, p. 5.

[3] B.L. Ioffe, V.A. Khoze and L.N. Lipatov: "Hard Processes" (North Holland, 1983).

[4] L.V. Gribov, Yu.L. Dokshitzer, V.A. Khoze and S.I. Troyan: Phys. Lett. **B202**, 276 (1988).

[5] L.V. Gribov, Yu.L. Dokshitzer, S.I. Troyan and V.A. Khoze: Yad. Fiz. **94**, 12 (1988); Sov. Phys. JETP **68**, 1303 (1988).

[6] D. Amati and G. Veneziano: Phys. Lett. **B83**, 87 (1979).

[7] Ya.I. Azimov, Yu.L. Dokshitzer, V.A. Khoze and S.I. Troyan: Z. Phys. **C27**, 65 (1985); Z. Phys. **C31**, 213 (1986).

[8] Yu. Dokshitzer and S. Troyan: "Nonleading Perturbative Corrections to the Dynamics of Quark-Gluon Cascades and Soft Hadron Spectra in e^+e^- Annihilation", preprint LNPI 922 (1984).

[9] Yu. Dokshitzer, V. Khoze, A. Mueller and S. Troyan: "Basics of Perturbative QCD" (Editions Frontières, 1991).

[10] OPAL Collaboration (M.Z. Akrawy et al.): Phys. Lett. **B247**, 617 (1990).

[11] L3 Collaboration (B. Adeva et al.): Phys. Lett. **B259**, 199 (1991).

[12] Yu. Dokshitzer, V. Khoze and S. Troyan: Z. Phys. **C55**, 107 (1992).

[13] J.G. Morfin and Wu-Ki Tung: Z. Phys. **C52**, 13 (1991).

[14] M. Glück, E. Reya and A. Vogt: Z. Phys. **C53**, 127 (1992).

[15] Ya. Azimov, Yu. Dokshitzer, V. Khoze and S. Troyan: Phys. Lett. **B165**, 147 (1985).

[16] OPAL Collaboration (M.Z. Akrawy et al.): Phys. Lett. **B261**, 334 (1991).

[17] G. Ingelman: "LEPTO 6.1 - The Lund Monte Carlo for Deep-Inelastic Lepton-Nucleon Scattering" in Proceedings of the Workshop on "Physics at HERA", DESY, Hamburg, Germany, 29-30 October 1991 (Ed. W. Buchmüller and G. Ingelman), vol. 3, p. 1366, and preprint TSL ISV 92-0065 (1992).

[18] ZEUS Collaboration (M. Derrick et al.): "The ZEUS Detector: Status Report 1989", DESY PRC 89-01 (March 1989).

FIGURE CAPTIONS

Fig. 1: Fractional momentum ($y_p = \ln(2p_h/Q)$) distributions of charged hadrons in the CF region of DIS at different Q^2 values: $Q^2 = 10^2$ GeV^2 (solid line), $Q^2 = 10^3$ GeV^2 (dashed line), $Q^2 = 10^4$ GeV^2 (dotted line) and $Q^2 = 10^5$ GeV^2 (dash-dotted line).

Fig. 2: Fractional momentum ($y_p = \ln(2p_h/Q)$) distributions of charged hadrons in the TF region of DIS at fixed Q^2: a) $Q^2 = 10^2$ GeV^2, b) $Q^2 = 10^3$ GeV^2 and c) $Q^2 = 10^4$ GeV^2, for different x values: $x = 10^{-2}$ (solid line), $x = 10^{-3}$ (dashed line) and $x = 10^{-4}$ (dotted line). The corresponding CF distributions (from Fig. 1), at the same Q^2 values, are also shown for comparison (dash-dotted line).

Fig. 3: Fractional momentum ($y_p = \ln(2p_h/Q)$) distributions of charged hadrons in the TF region of DIS at fixed x: a) $x = 10^{-2}$ and b) $x = 10^{-3}$, for different Q^2 values: $Q^2 = 10^2$ GeV^2 (solid line), $Q^2 = 10^3$ GeV^2 (dashed line) and $Q^2 = 10^4$ GeV^2 (dotted line).

Fig. 4: Fractional momentum ($y_p = \ln(2p_h/Q)$) distributions of charged hadrons in the TF region of DIS at different Q^2 and x values: a) $Q^2 = 10^2$ GeV^2, $x = 10^{-3}$ and b) $Q^2 = 10^3$ GeV^2, $x = 10^{-2}$, using two different sets of structure functions: S-DIS [13] (solid line) and GRV(HO) [14] (dashed line).

Fig. 5: Monte Carlo simulations of the fractional momentum ($y_p = \ln(2p_h/Q)$) distributions of charged pions in the TF region of DIS at fixed $x = 10^{-2}$, for different Q^2 values: $Q^2 = 10^2$ GeV^2 (solid line) and $Q^2 = 10^3$ GeV^2 (dashed line).

Fig. 6: Monte Carlo simulations of the fractional momentum ($y_p = \ln(2p_h/Q)$) distributions of charged pions in the TF region of DIS at fixed $Q^2 = 10^2$ GeV^2, for different x values: $x = 10^{-2}$ (solid line) and $x = 10^{-3}$ (dashed line).

Fig. 7: Monte Carlo simulations of the fractional momentum ($y_p = \ln(2p_h/Q)$) distributions of charged pions in the CF region of DIS at different Q^2 and x values: $Q^2 = 10^2$ GeV^2, $x = 10^{-2}$ (solid line), $Q^2 = 10^2$ GeV^2, $x = 10^{-3}$ (dashed line) and $Q^2 = 10^3$ GeV^2, $x = 10^{-2}$ (dotted line).

Fig. 8: Monte Carlo simulations of the fractional momentum ($y_p = \ln(2p_h/Q)$) distributions of charged pions in the TF region of DIS at different Q^2 and x values: a) $Q^2 = 10^3$ GeV^2, $x = 10^{-2}$ and b) $Q^2 = 10^2$ GeV^2, $x = 10^{-3}$, relative to the full phase-space

(solid line) and accounting for the forward hole on the outgoing proton side of the ZEUS detector at HERA (dashed line).

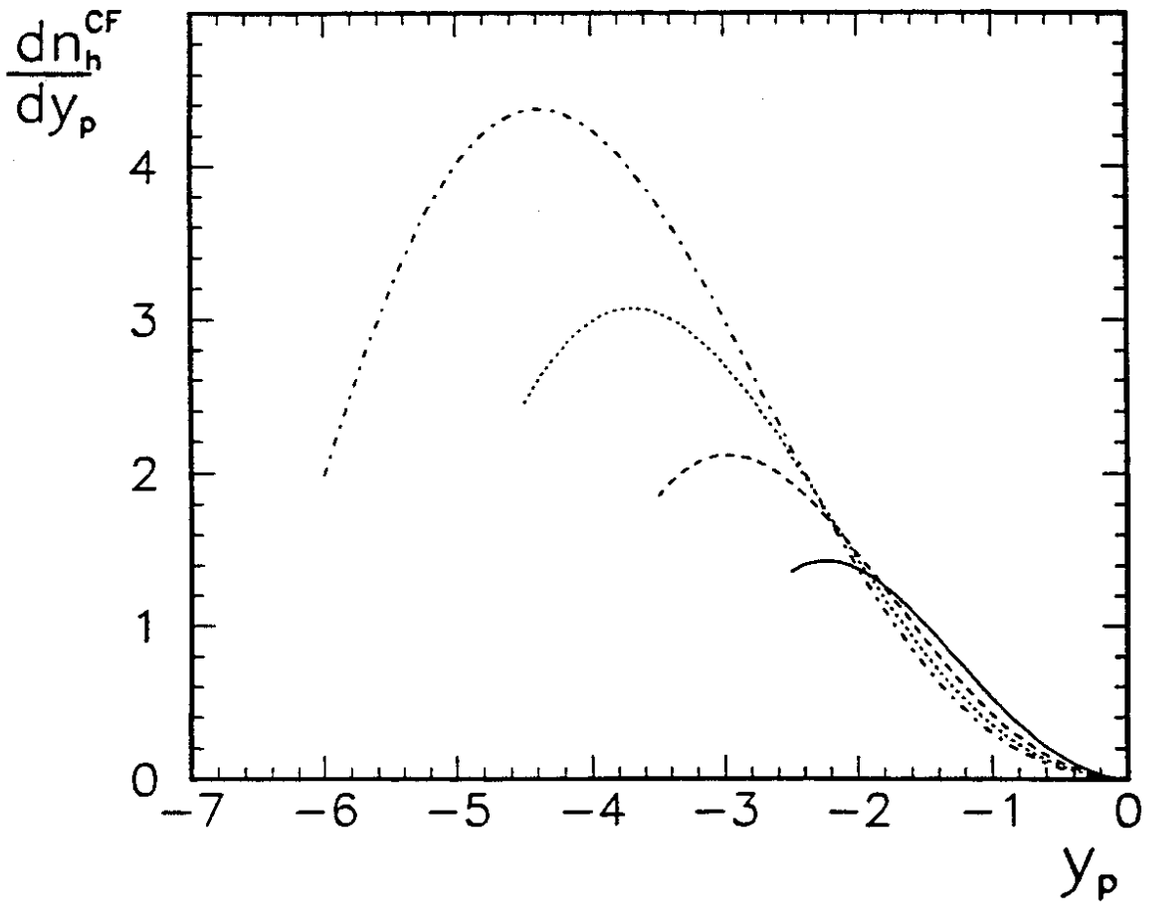

Fig. 1

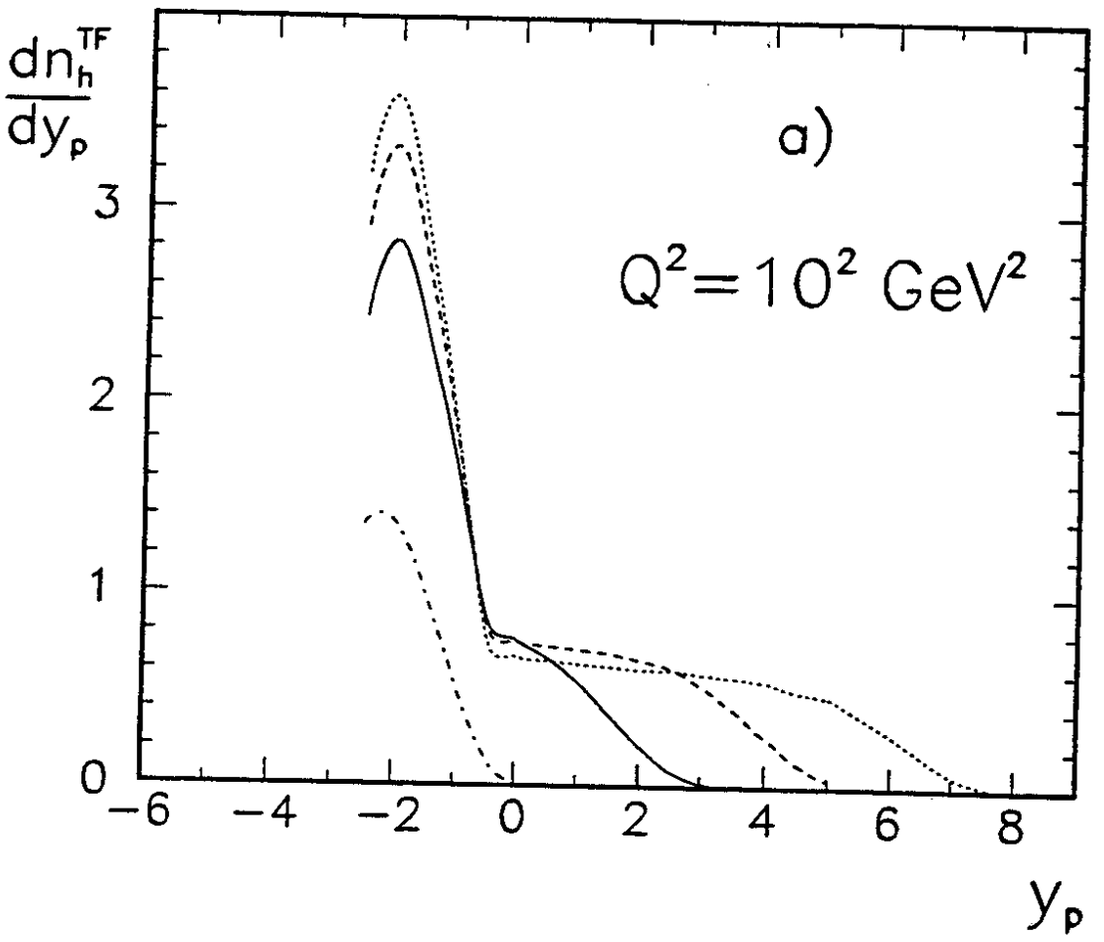

Fig.2a

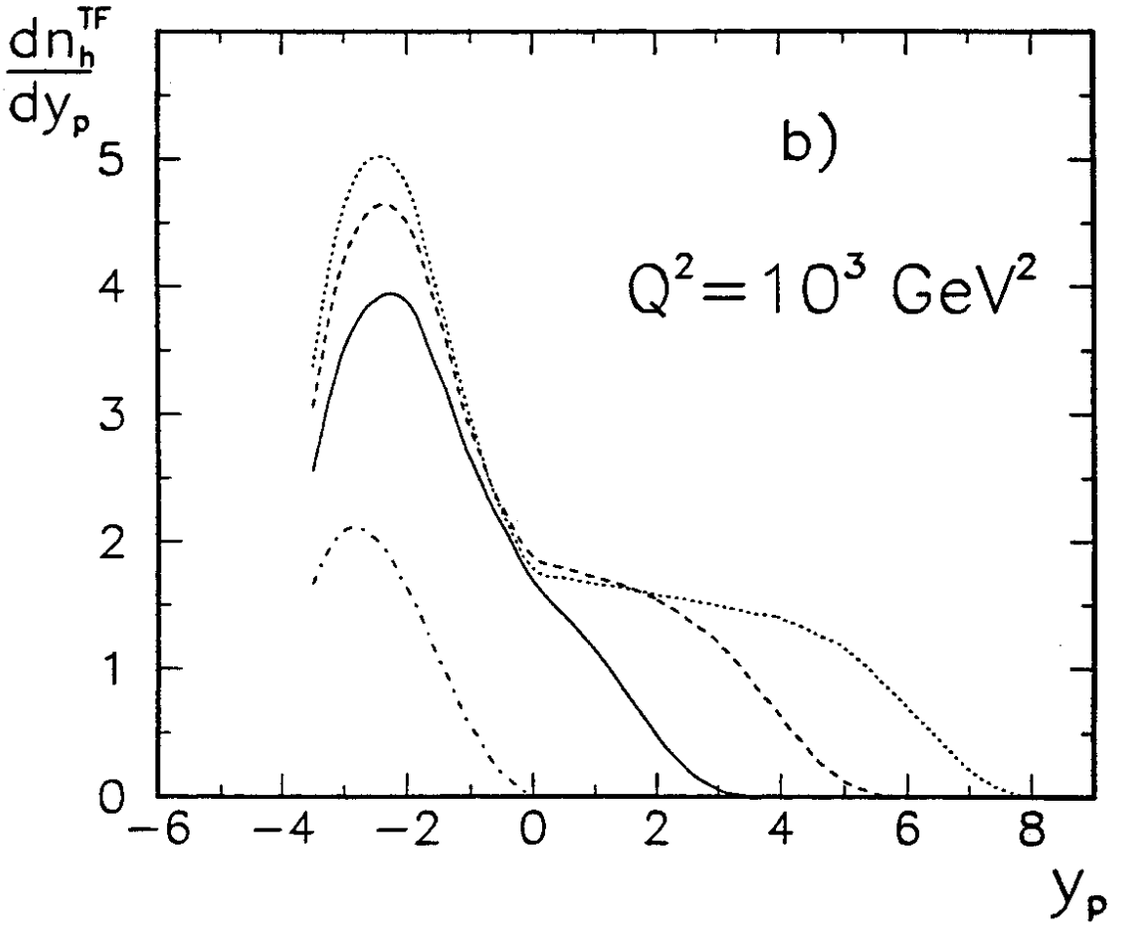

Fig.2b

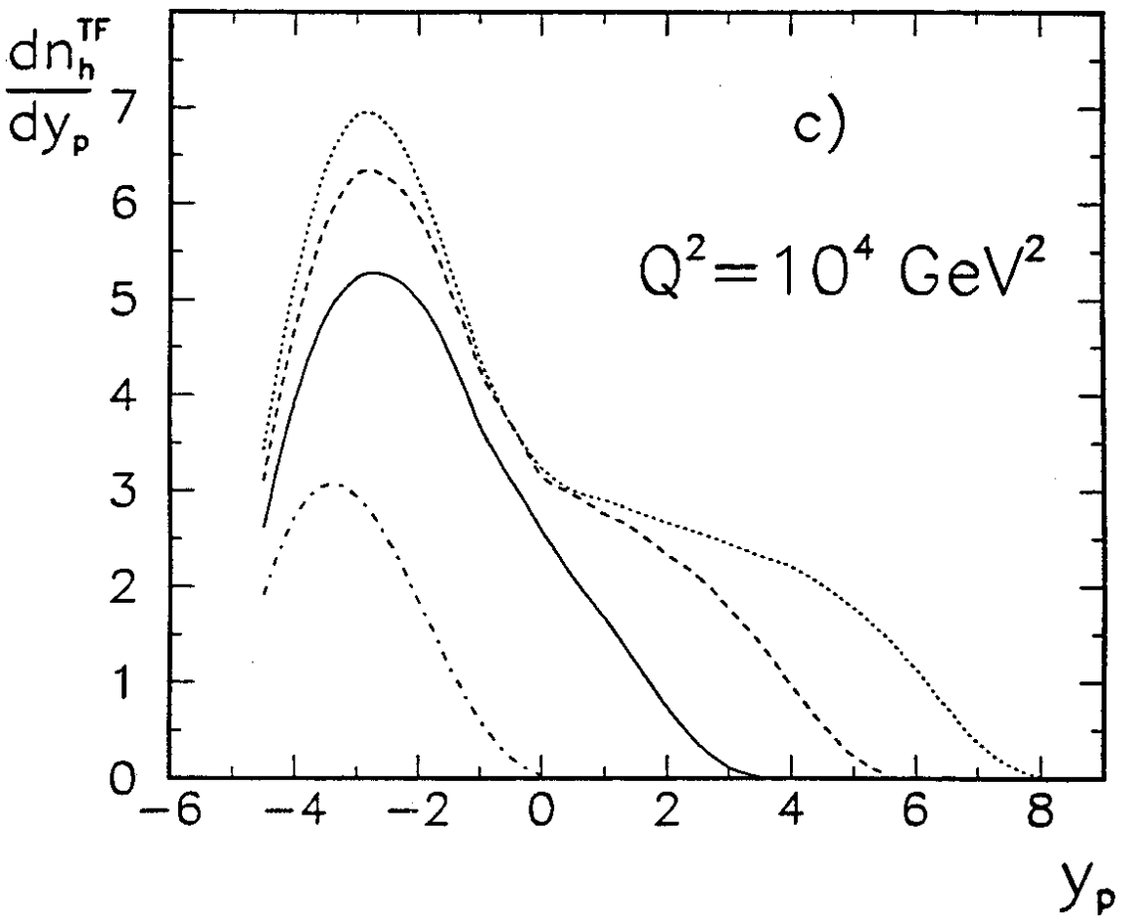

Fig.2c

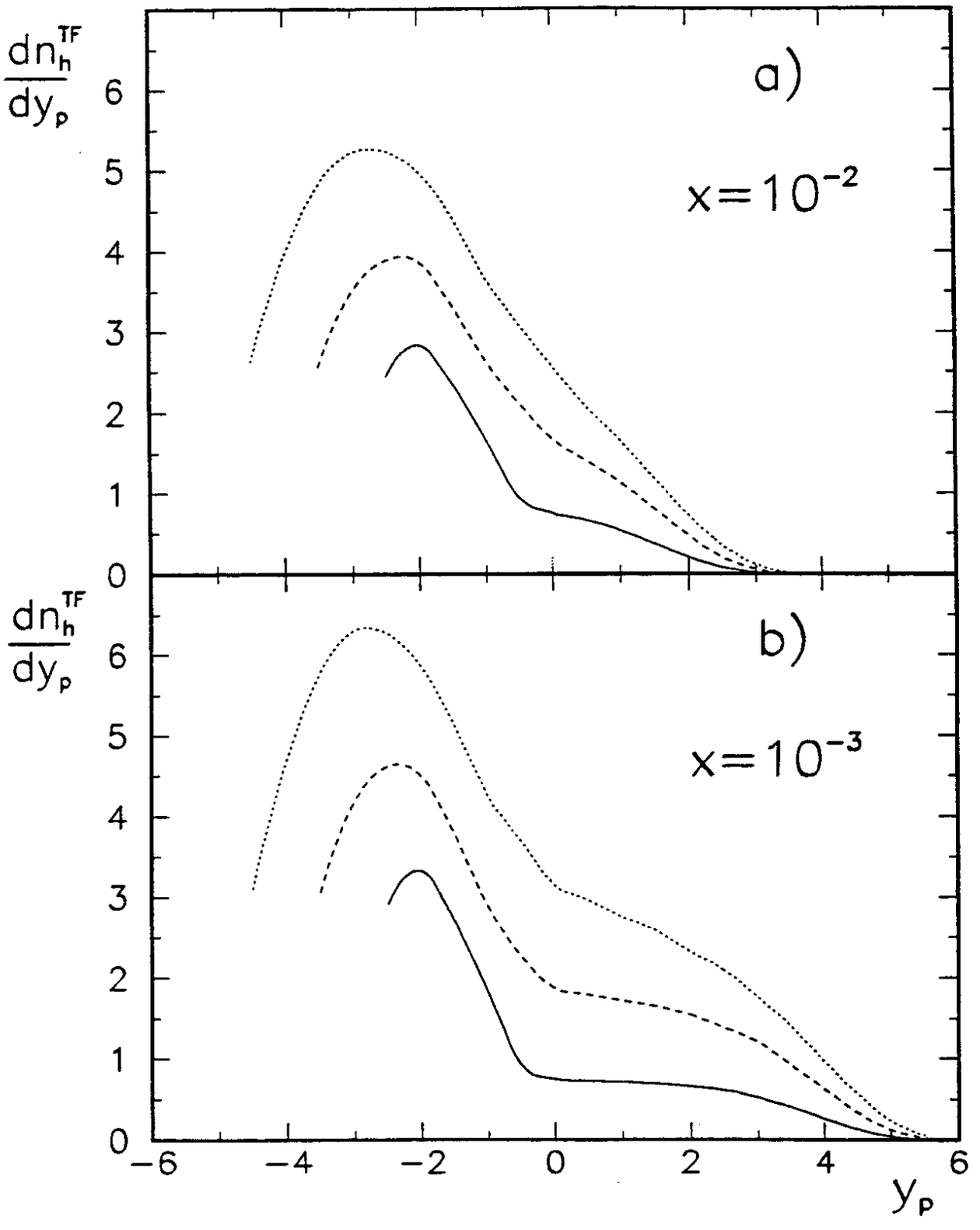

Fig.3

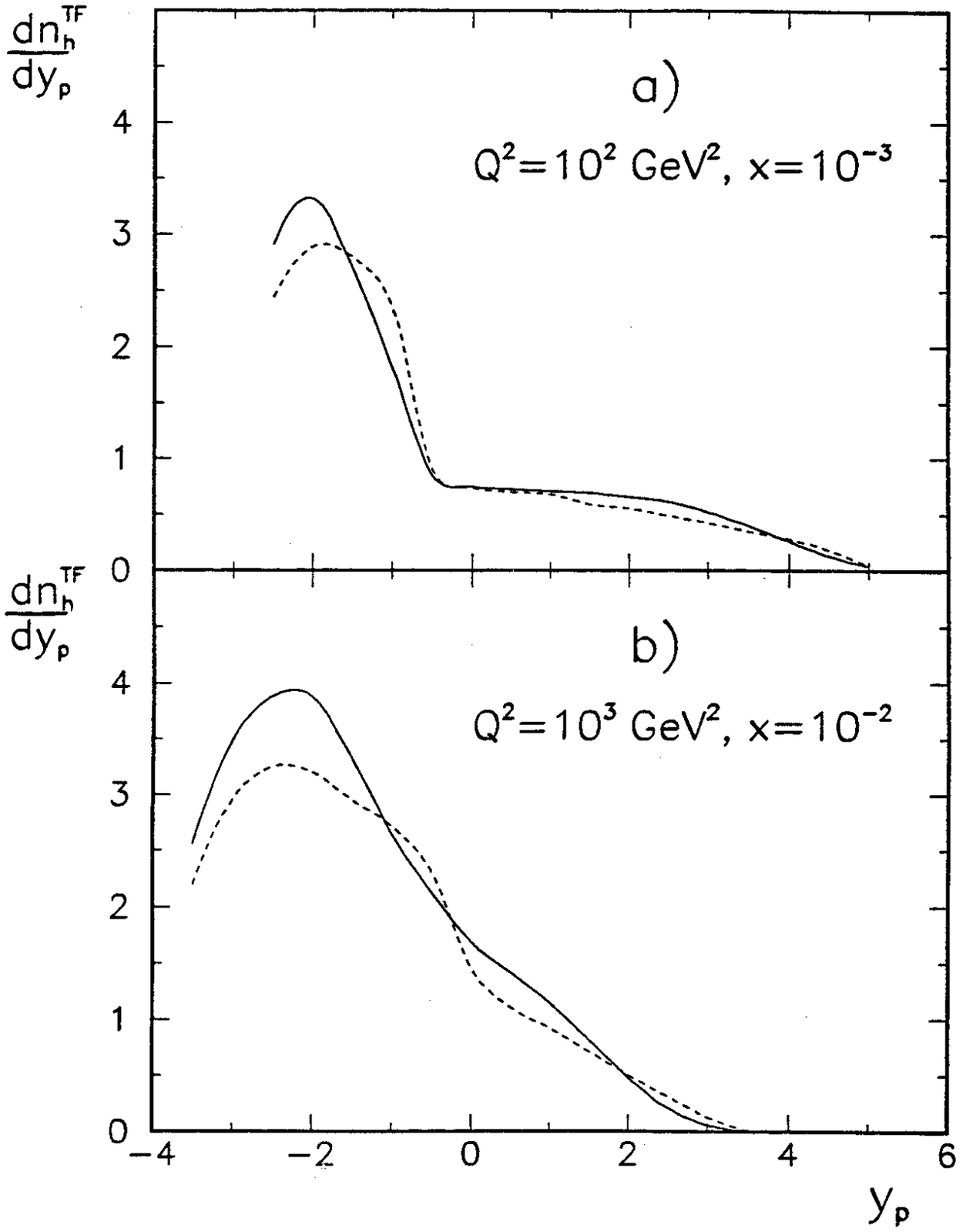
$\frac{dn_h^{TF}}{dy_p}$
a)
$Q^2=10^2$ GeV^2, $x=10^{-3}$
$\frac{dn_h^{TF}}{dy_p}$
b)
$Q^2=10^3$ GeV^2, $x=10^{-2}$
0
1
2
3
4
−4
−2
0
2
4
6
y_p

Fig.4

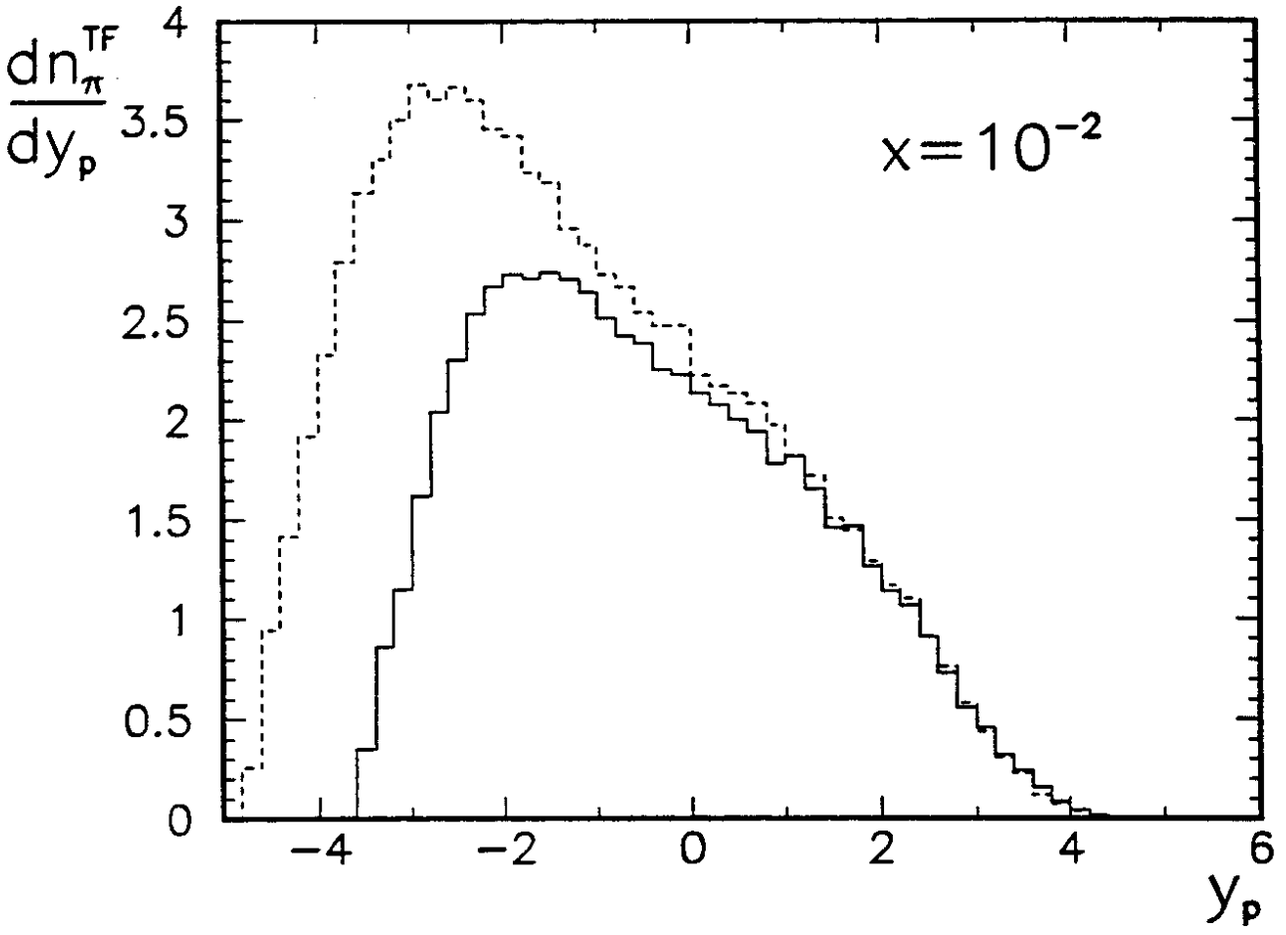

Fig. 5

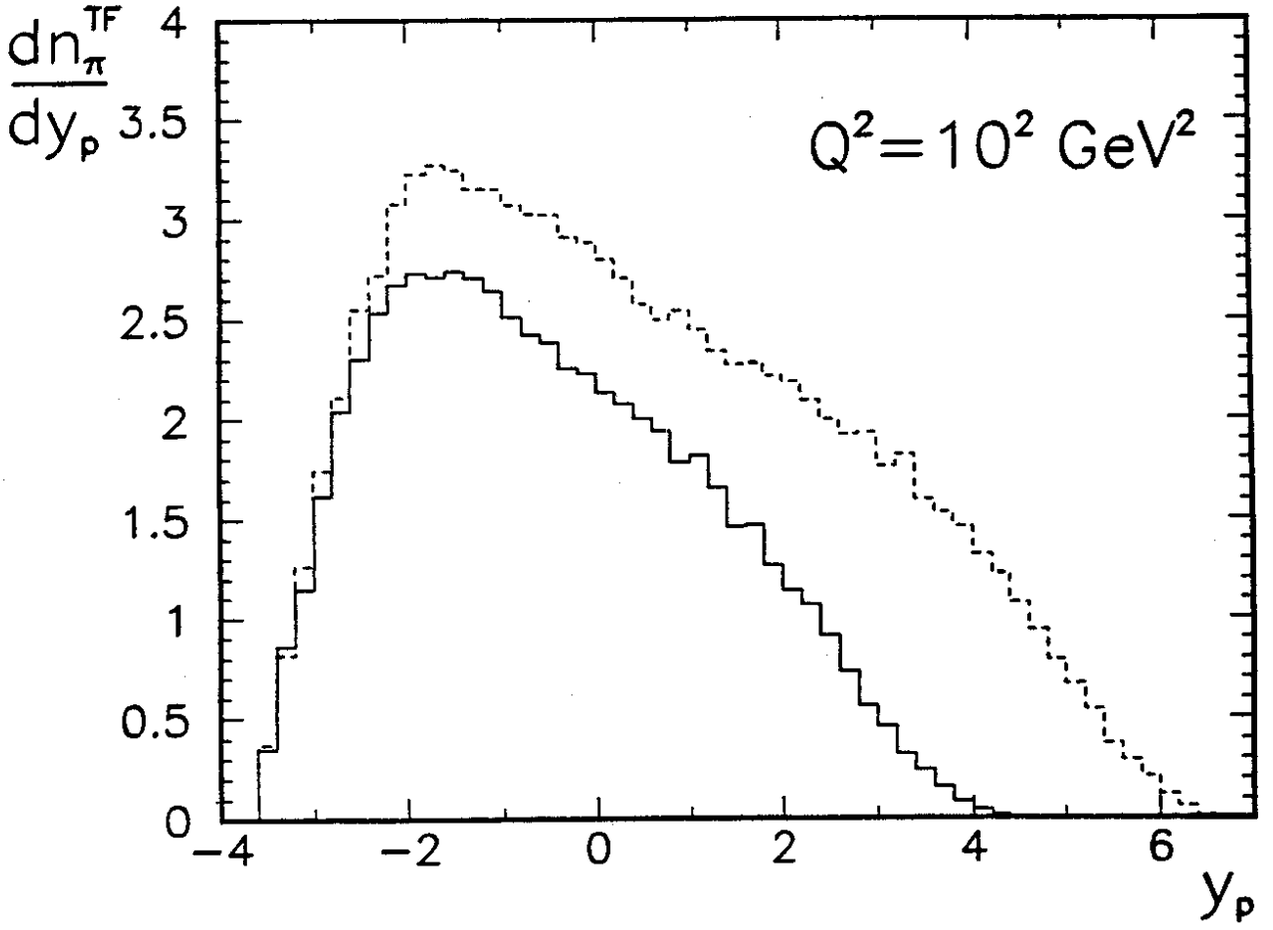

Fig. 6

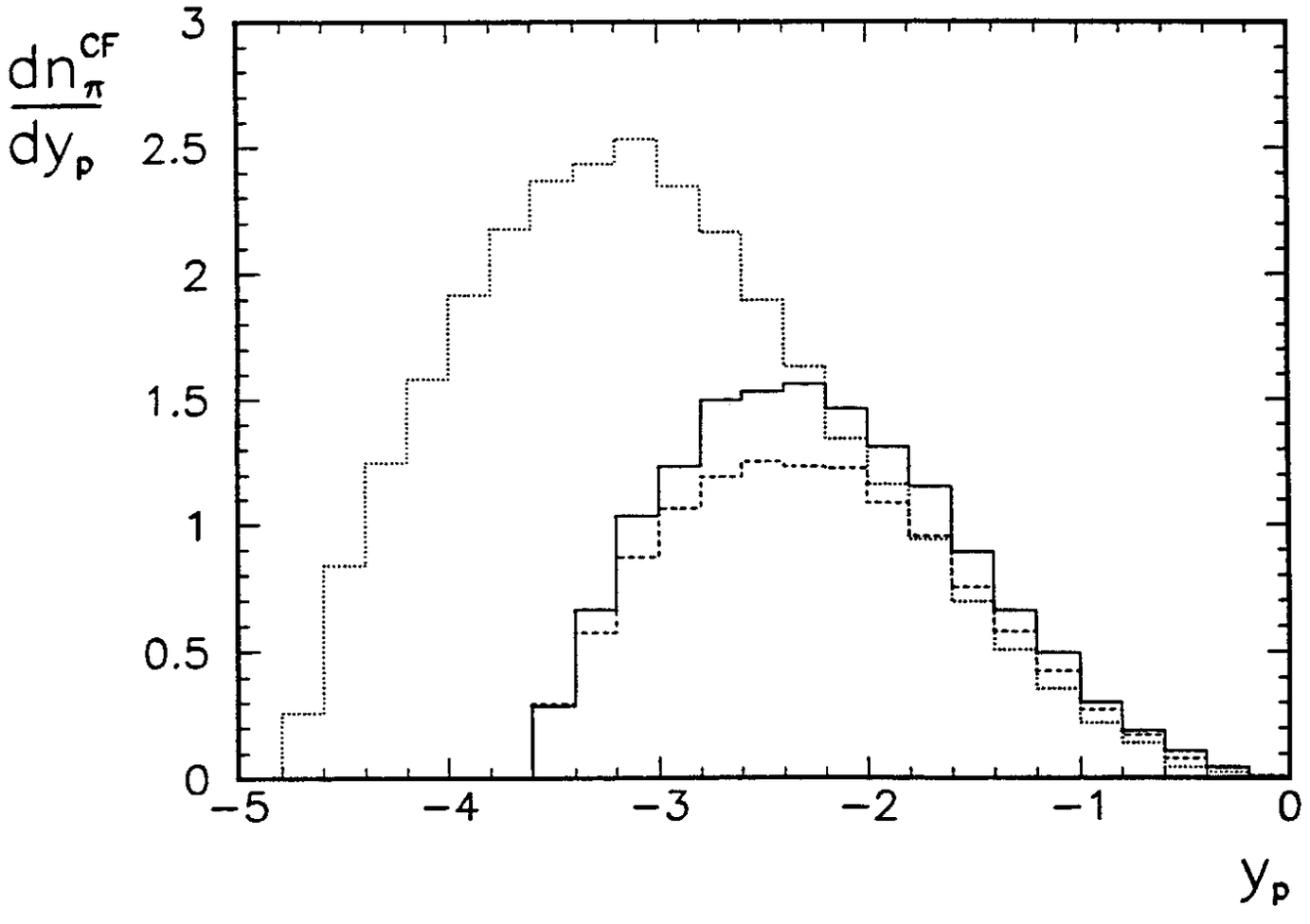

Fig. 7

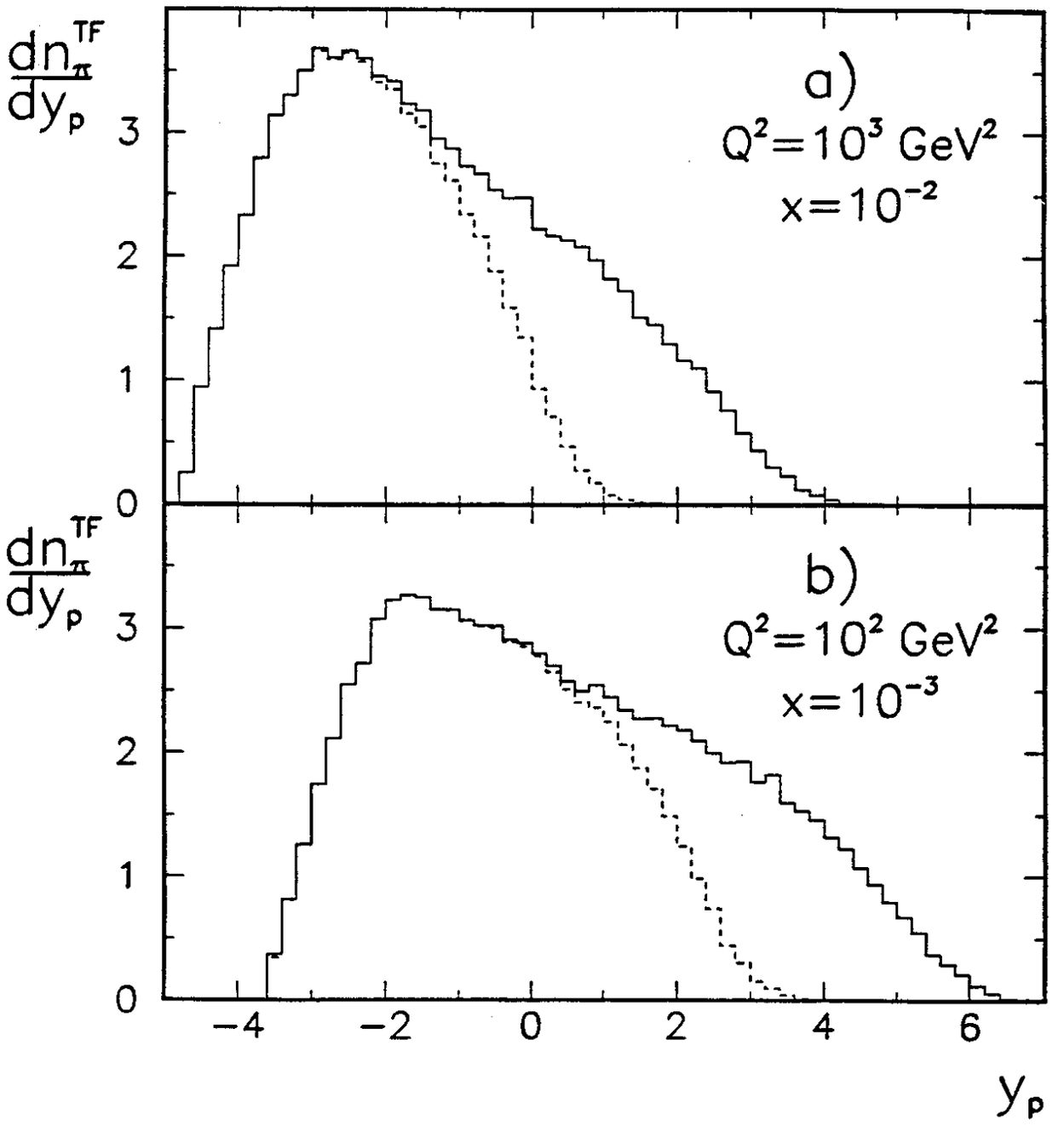
$\frac{dn_\pi^{TF}}{dy_p}$
a)
$Q^2=10^3$ GeV^2
$x=10^{-2}$
b)
$Q^2=10^2$ GeV^2
$x=10^{-3}$
0
1
2
3
−4
−2
0
2
4
6
y_p

Fig. 8